Journal of Solid State Electrochemistry
https://doi.org/10.1007/s10008-023-05695-4

SHORT COMMUNICATION

Solid electrolytes based on zirconium dioxide partially stabilized with oxides of yttrium, gadolinium, and samarium

D. A. Agarkov[1,3] · M. A. Borik[2] · A. S. Chislov[2,4] · B. E. Komarov[2] · A. V. Kulebyakin[2] · I. E. Kuritsyna[1] · E. E. Lomonova[2] · F. O. Milovich[4,5] · V. A. Myzina[2] · N. Yu. Tabachkova[2,4]

Received: 5 September 2023 / Revised: 18 September 2023 / Accepted: 19 September 2023

Abstract

The phase composition, structure, conductivity, crack resistance, and microhardness of crystals $(ZrO_2)_{1-x}(R_2O_3)_x$, where R = Y, Gd, Sm, and (x = 0.03, 0.04, 0.05) were studied. Crystals were grown by directed crystallization of the melt in a cold crucible. Crystals were studied by X-ray diffraction, transmission electron microscopy, impedance spectroscopy, and indentation. The concentration dependences of the investigated characteristics of crystals are obtained. It has been shown that an increase in the concentration of the stabilizing oxide in all cases leads to a decrease in the amount of the transformed t-phase and reduces the value of the crack resistance of the crystals. In this case, a decrease in the size of the twins and an increase in the defectiveness of the structure are observed, which is accompanied by a slight decrease in the electrical conductivity of tetragonal solid solutions. The influence of the ionic radius of trivalent cations on the stabilization of tetragonal phases, conductivity, and the mechanical properties of crystals is discussed. An increase in the values of crack resistance and a decrease in the values of high-temperature electrical conductivity of tetragonal solid solutions in the series $Y_2O_3 \rightarrow Gd_2O_3 \rightarrow Sm_2O_3$ at comparable concentrations of stabilizing oxides were established. It has been shown that ZrO_2 solid solutions stabilized with Sm_2O_3 can be used as functional supporting membranes in solid oxide fuel cells.

Keywords Zirconia membranes · SOFC · Single crystal · Structure · Conductivity

Introduction

Materials based on zirconia are solid electrolytes with oxygen ion conductivity, the properties of which have been studied for many years. The results of these studies led to the creation of heating elements, oxygen sensors, solid oxide fuel cells, oxygen pumps, electrolyzers for hydrogen production, etc. on their basis [1–5]. In such devices, solid solutions based on zirconium dioxide can be used in the form of ceramics, films, and single crystals. The properties of materials even with the similar composition may differ in performance and stability when operating under different conditions [6–8]. This is due to the quality of the starting materials, synthesis methods, and heat treatment conditions.

The active layers (anode, cathode, electrolyte) of modern electrochemical devices' cell designs are, as a rule, approximately 10–150-μm thin, which ensures high power density at operating temperature. However, the use of thin active layers requires a structurally supporting layer, which can be one of the functional layers of the device. For further development and scaling of the technologies of solid oxide fuel cells and electrolyzers, it is essential to increase the mechanical strength of these components.

As a rule, cubic solid solutions based on zirconium dioxide, which have the highest conductivity, are used as solid electrolyte membranes. However, they have very low

✉ D. A. Agarkov
agarkov@issp.ac.ru

1 Osipyan Institute of Solid State Physics RAS, Academician Osipyan Str, 2, 142432 Chernogolovka, Moscow District, Russia

2 Prokhorov General Physics Institute of Russian Academy of Sciences, Vavilova Street, 38, 119991 Moscow, Russia

3 Moscow Institute of Physics and Technology, Institutsky Lane, 9, 141700 Dolgoprudny, Moscow Region, Russia

4 Department of Materials Science of Semiconductors and Dielectrics, National University of Science and Technology "MISIS", Leninskiy Prospekt, 4, 119049 Moscow, Russia

5 Department of Materials Science, Moscow Polytechnic University, Bolshaya Semyonovskaya Street, 38, 107023 Moscow, Russia

Published online: 30 September 2023

resistance to thermal shocks and are typical brittle materials that, despite high microhardness, have low crack resistance of ~ 1 to 3 MPa·$m^{1/2}$ [9–11]. An alternative material that can be used as solid electrolyte membranes is partially stabilized zirconia, which combines high hardness, strength, and fracture toughness [12–14]. The combination of such characteristics with high conductivity in a material is important for ensuring the reliability of the design of an electrochemical device and increasing its service life [15–18].

Zirconium dioxide has several polymorphic modifications [19]. At atmospheric pressure, monoclinic (m—$P2_1/C$), tetragonal (t—$P4_2/nmc$), and cubic (c—Fm3m) modifications are known for ZrO_2, which exist in different temperature ranges. Due to the destructive monoclinic-tetragonal phase transition (Tm ↔ t ~ 1473 K), pure zirconium dioxide is practically not used. However, it has been established [9–11] that the effect of this transformation transition can be eliminated by adding oxides of rare earth elements, yttrium, scandium, and oxides of alkaline earth oxides to zirconium dioxide. The degree of stabilization depends on the nature of the stabilizing oxide and its concentration. When a stabilizing oxide is introduced into zirconium dioxide, according to crystal chemical concepts, stable solid solutions can appear. Cubic solid solutions based on zirconia, stable up to the melting point, are called fully stabilized zirconia (FSZ). With a decrease in the concentration of the stabilizing oxide, solid solutions with a tetragonal structure are obtained. Since the upper temperature limit of the phase stability of these tetragonal solid solutions is the tetragonal-cubic phase transition temperature, and it is below the melting point, such materials are called partially stabilized zirconia (PSZ). With a further decrease in the concentration of the stabilizing oxide in the tetragonal solid solution, a monoclinic phase can appear. The formation of point defects in the crystal lattice, for example, oxygen vacancies, leads to the stabilization of the high-temperature phase, creating a potential barrier to the movement of the interface. Such a process occurs when zirconium dioxide is stabilized by metal oxides with cations of a lower valence than that of zirconium. Thus, when yttrium oxide is introduced, there is one oxygen vacancy per two introduced trivalent Y^{3+} ions. This contributes not only to the possibility of stabilizing the high-temperature modification of zirconium dioxide, but also makes this material an effective oxygen ion conductor.

There are two forms of tetragonal ZrO_2 [9–14]: "non-transformable" t'-ZrO_2 rich in yttrium oxide and t-ZrO_2 depleted in yttrium oxide, which is capable of undergoing a martensitic transition to the monoclinic phase—m. In the ZrO_2-Y_2O_3 phase diagram, in the concentration range rich in zirconium dioxide, the existence regions of the cubic and tetragonal phases are separated by a two-phase region (c + t). The cubic-tetragonal and tetragonal-monoclinic phase transitions in zirconium dioxide and solid solutions based on it have been studied in a number of works [20–22]. Phase transitions in zirconium dioxide are accompanied by the formation of twins in the structure, which fill the entire volume of the crystal grain. Twinning is the result of optimal accommodation of spontaneous stresses caused by a phase transition from a cubic to a tetragonal phase [23]. The value of tetragonality depends on the composition of the solid solution.

To explain the high mechanical characteristics of partially stabilized zirconium dioxide, the mechanisms of "transformational" and ferroelastic hardening were proposed [7–10].

The action of the mechanism of transformation hardening was explained by the fact that the emerging microcrack induces a martensitic t → m transition, which absorbs the stress energy at its tip. When a monoclinic phase appears, the propagating microcrack is compressed due to the larger specific volume of the monoclinic phase compared to the tetragonal one. For these reasons, in the end, the propagation of microcracks stops. The martensitic transformation of the tetragonal phase into a monoclinic phase at low temperatures provides an increased fracture toughness of ceramics based on this type of zirconium dioxide [24].

A number of authors [9–12] associate the hardening mechanism with a ferroelastic transformation caused by the transition of a cubic phase to a tetragonal one. It is known, that ferroelastic properties are possessed by a material that has two or more stable orientational states and is capable of transitioning from one state to another when a mechanical load is applied. The ferroelastic properties of tetragonal zirconium dioxide appear due to the symmetry-lowering phase transition of the initial cubic phase into the tetragonal phase (t'), which causes three energetically equivalent orientational states, also called twin variants or domains. When loaded, the domains can reorient their axes to accommodate stresses. The details of this effect have been studied by a number of authors [11, 25]. The twinned structure depends on the direction and type of loading, as well as on the orientation of the crystal and domain switching in ferroelastic materials.

Thus, several different strengthening mechanisms for partially stabilized zirconia have been proposed. At the same time, it is obvious that they act in materials of partially stabilized zirconium dioxide under different loading conditions in different ways: either the action of one of the hardening mechanisms can prevail, or the action of several can be effective. It was shown [9–12, 26] that ferroelastic hardening should be considered as a possible mechanism of hardening at elevated temperatures, since the effect of transformation hardening is limited by the phase transition t → m temperature, which decreases significantly with the introduction of a stabilizing impurity [26].

Ceramic materials of partially stabilized zirconia 3YSZ were studied as electrolytic membranes in SOFCs instead of the traditional solid electrolyte based on zirconia

containing 8 mol% yttria [15]. It was shown that due to the improvement of mechanical characteristics, it is possible to reduce the thickness of the electrolyte from 150 to 75 μm, which improves the cell performance associated with a decrease in ohmic resistance. The authors see further prospects in optimizing the composition and microstructure of the material, both electrolyte and anode and cathode materials.

In recent years, most commonly planar SOFCs have an anode supported cell design consisting of a thick Ni/YSZ substrate, a thin Ni/YSZ fuel electrode, a thin YSZ electrolyte layer, and a thin YSZ/lanthanum strontium manganite (LSM) cathode [16]. The reliability of this design largely depended on the strength characteristics of the YSZ. It has been established that lowering the concentration of the stabilizing oxide below 5.8 mol% $YO_{1.5}$ can improve the fracture toughness of membranes under oxidizing conditions by increasing the phase transformation ability of tetragonal zirconia. A decrease in the concentration of yttrium oxide contributes to an increase in the efficiency of the transformation hardening mechanism. To ensure the stability of mechanical characteristics at operating temperatures (1073 K), in [16], co-doping with yttrium and cerium oxides was used. It has been established that the composition $1.5CeO_2$ $4.5YO_{1.5}$-SZ provides increased fracture toughness and resistance to low-temperature and high-temperature degradation (LTD and HTD) of the support layer in a solid oxide fuel cell or electrolysis cell support [16].

The study of the transport characteristics of partially stabilized zirconia, which has high strength, fracture toughness, and hardness has a great interest. The aim of this work is the synthesis and comparative study of the mechanical and transport characteristics of zirconium dioxide crystals partially stabilized by yttrium, gadolinium, and samarium oxides. The use of partially stabilized zirconium dioxide crystals grown by directional melt crystallization in a cold container as an object of study makes it possible to compare the structure of materials, mechanical and transport characteristics depending on the type and concentration of the stabilizing oxide. In ceramic materials, comparison of these characteristics of materials based on zirconium dioxide is impossible without taking into account the influence of grain size on them, grain boundaries, and segregation of impurities in the grain and at the boundaries. The significant influence of these factors on the comparison results can lead to contradictory or conflicting results. When using crystals, we obtain bulk characteristics of the material that are close to those of ceramic grains of the same composition. When grown from a melt at a crystallization temperature, a single crystal grows with a cubic lattice structure. As it cools, phase transformations take place in the corresponding temperature ranges.

Materials and methods

Crystals of solid solutions based on zirconium dioxide, $(ZrO_2)_{1-x}(Y_2O_3)_x$, $(ZrO_2)_{1-x}(Gd_2O_3)_x$, and $(ZrO_2)_{1-x}(Sm_2O_3)_x$ at $x = 0.03$, 0.04, and 0.05, were grown by the method of directed melt crystallization in a cold container [27]. Further in the text, short designations of crystals xYSZ, xGdSZ, and xSmSZ are used, where x is the concentration of the stabilizing oxide in mol%. The growth of crystals of different compositions was carried out under the same conditions. The starting materials used were oxides of zirconium, yttrium, gadolinium, and samarium of high-purity grade with a purity of at least 99.99%. The powders of the initial oxides were weighed and mechanically mixed beforehand. The mixture of powders was placed in a cylindrical split container consisting of a set of copper tubes cooled with water. Metallic zirconium was used for initial melting, which, when heated by a high-frequency field, oxidized with heat release, heating the surrounding charge. When heated, this part of the load became electrically conductive enough to directly absorb the energy of the high-frequency field. The formed volume of the melt was the starting one and gradually spread to the walls of the cold container. A layer of sintered, unmelted charge was preserved on the walls, the so-called garnissage, which prevents the melt from flowing out and ensures the purity of the crystallized melt. Loading weight in all melts was 5 kg. The growth was carried out on a Kristall-407 high-frequency setup at an operating frequency of 5.28 MHz and a cold container diameter of 120 mm. The growth rate of crystals is 10 mm/hour.

The phase composition of the crystals was studied using X-ray diffraction with a Bruker D8 instrument using the standard method for single crystals. The as-grown crystals had no predominant crystallographic orientation. Therefore, each crystal was preliminarily oriented along specific crystallographic directions in the diffractometer. Then, the crystals were cut into plates on a diamond disc cutting machine. The phase composition of the crystals was studied for plates cut from the crystals perpendicular to the <100> direction. The {100} planes of the crystals that had a multiphase composition exhibited simultaneous reflections on a single cut that were produced by different phases; these reflections split at large 2θ values of ~ 130 arc degrees. The phase fractions were determined from the diffraction peak intensities normalized to the integral reflection coefficients of the different phases. The crystal microstructure was studied using a JEM 2100 transmission electron microscope at an accelerating voltage of 200 kV.

The microhardness of a material characterizes its ability to resist being pressed into it by another body or scratched. Hardness is not a physical constant of a substance but is a property that depends not only on the characteristics

of the sample, but also on the method of measurement. The microhardness of crystals was studied on the basis of a motorized microhardness tester DM 8 V AUTO using a Vickers diamond tetrahedral pyramid and loads up to 20 N. A load of 3 N was chosen as a load for studying microhardness.

The fracture toughness was estimated from the value of the critical stress intensity factor (K_{1c}), which was determined by the Vickers indentation method. To calculate K_{1c}, the Niihara formula for the Palmquist fracture system was used [28–30]:

$$K_{1c} = 0.035(L/a)^{-1}(CE/H)^{2/5}Ha^{1/2}C^{-1}$$

where K_{1c} is the stress intensity factor (MPa·m$^{1/2}$); L is the length of the radial crack (m); a is the indentation half-width (m); C is the Poisson's ratio; E is Young's modulus, Pa; and H is microhardness, Pa.

K_{1c} was calculated for radial cracks around the indent, the length of which met the criterion of $0.25 \le l/a \le 2.5$ for Palmquist cracks. The studies were carried out on a Wolpert Hardness Tester 930 with a minimum load of 50 N. To study the crack resistance, the load used was 100 N.

The transport characteristics of the crystals were studied by impedance spectroscopy on a Solartron SI 1260 analyzer. The temperature range of measurements was 673–1173 K with a step of 50 K, the frequency range in which measurements were taken was 1–5 MHz. The measurements were carried out on plates cut from crystals. The dimensions of the samples were $7 \times 7 \times 0.5$ mm. Symmetrical platinum electrodes were deposited on a large surface (7×7) mm of the plates. To do this, platinum paste was applied to the plates and annealed at a temperature of 1223 K for 1 h in air. The amplitude of the applied alternating signal to the sample was 24 mV. A detailed analysis of the frequency spectrum of the impedance was carried out using the ZView program. The resistances of solid electrolytes were calculated from the obtained impedance spectra, and then, the electrical conductivity of the crystals was calculated.

Results and discussion

Phase composition of crystals

Table 1 shows the phase composition, weight fraction of phases, and the degree of tetragonality of solid solutions of $(ZrO_2)_{1-x}(Y_2O_3)_x$, $(ZrO_2)_{1-x}(Gd_2O_3)_x$, and $(ZrO_2)_{1-x}(Sm_2O_3)_x$ at $x = 0.03$, 0.04, and 0.05.

At a stabilizing oxide concentration of 3 mol%, the phase composition of the crystals differs. Thus, in 3YSZ and 3GdSZ crystals, two tetragonal phases with different degrees of tetragonality are formed. 3SmSZ crystals contain a mixture of monoclinic and tetragonal ZrO_2 modifications. Thus, when Sm_2O_3 is used as a stabilizer, a concentration of 3 mol% is insufficient for stabilizing tetragonal phases in the entire volume of the crystal. At concentrations of 4 mol% and 5 mol% of the stabilizing oxide, two tetragonal phases were present in all the crystals under study. Since the implementation of the mechanism of transformation hardening depends on the amount of the transformed tetragonal phase (t) and the transformation ability of this phase, it is important to note that at comparable concentrations of the stabilizing oxide, the amount of the transformed phase (t) increases in the series $Y_2O_3 \rightarrow Gd_2O_3 \rightarrow Sm_2O_3$. The degree of tetragonality of the transformed phase also depends on the type of stabilizing oxide and also increases in the series $Y_2O_3 \rightarrow Gd_2O_3 \rightarrow Sm_2O_3$. This regularity correlates with the change in the ionic radius of the stabilizing oxide cation. The ionic radii of Y^{3+}, $Gd^{3}+$, and Sm^{3+} for a coordination number of 8 are 1.019 Å, 1.053 Å, and 1.079 Å, respectively. The larger the ionic radius of the stabilizing oxide cation, the greater the amount of the tetragonal phase with a higher degree of tetragonality ($c/\sqrt{2}a$) is present in the crystals at comparable concentrations.

The different degree of tetragonality of the phases t and t' indicates that different amounts of the stabilizing oxide are dissolved in them. In this case, a decrease in the content of the stabilizing oxide in the t-phase leads to an increase in the degree of tetragonality of the transformed phase. For the

Table 1 Phase composition, weight fraction of phases, and degree of tetragonality of solid solutions

x, (mol%)	Y_2O_3			Gd_2O_3			Sm_2O_3		
	Phase	Fraction, wt.%	$c/\sqrt{2}a$	Phase	Fraction, wt.%	$c/\sqrt{2}a$	Phase	Fraction, wt.%	$c/\sqrt{2}a$
3	t	75 ± 5	1.0147	t	80 ± 5	1.0160	m	25 ± 5	1.0171
	t´	25 ± 5	1.0052	t´	20 ± 5	1.0059	t	75 ± 5	
4	t	65 ± 5	1.0143	t	70 ± 5	1.0151	t	85 ± 5	1.0167
	t´	35 ± 5	1.0049	t´	30 ± 5	1.0047	t´	15 ± 5	1.0034
5	t	55 ± 5	1.0139	t	60 ± 5	1.0148	t	75 ± 5	1.0158
	t´	45 ± 5	1.0044	t´	40 ± 5	1.0040	t´	25 ± 5	1.0031

non-transformable phase, a decrease in the degree of tetragonality will be associated with an increase in the content of the stabilizing oxide in the t'-phase. With the total same content of the stabilizing oxide in the crystals in the series $Y_2O_3 \rightarrow Gd_2O_3 \rightarrow Sm_2O_3$, not only the degree of tetragonality of the transforming phase increases, but also the degree of tetragonality of the non-transformable t'-phase decreases. This may be due to the lower content of the stabilizing oxide in the transformable phase and the higher content of the stabilizing oxide in the non-transformable phase.

Thus, at comparable total concentrations of stabilizing oxides in crystals, the use of a cation with a large ionic radius as a stabilizer leads to greater phase separation and brings the system closer to a more equilibrium state. It is possible that this is due to the fact that phase transformations during the transition from the cubic to the two-phase region in SmSZ crystals occur at higher temperatures than in GdSZ crystals, and in GdSZ crystals at higher temperatures than in YSZ crystals of the same composition.

The pattern of change in the weight fraction of phases and the degree of tetragonality in YSZ, GdSZ, and SmSZ solid solutions depending on the concentration of the stabilizing oxide is similar. With an increase in the concentration of stabilizing oxides, the amount of the transformable phase (t) decreases and the amount of the non-transformable phase (t`) increases. The degree of tetragonality ($c/\sqrt{2}a$) of phases decreases with increasing concentration of stabilizing oxides.

Microstructure

A detailed study of the crystal microstructure was carried out by transmission electron microscopy. Figure 1 shows images of the structure of YSZ, GdSZ, and SmSZ crystals with a stabilizing oxide concentration of 3 mol%.

All crystals contain twins. In this case, twins occupy the entire volume of the material; no regions free of twins were observed in the crystals under study. The shape of the electron diffraction patterns from different parts of the crystals always corresponded to the single-crystal diffraction pattern. For 3YSZ and 3GdSZ crystals, the arrangement of reflections in the electron diffraction patterns corresponded to the tetragonal modification of ZrO_2. For 3SmSZ crystals, regions with monoclinic and tetragonal ZrO_2 modifications were observed. At the same time, microcracks were sometimes present at the points of junctions of the monoclinic and tetragonal phases. The twin structure morphology for 3YSZ and 3GdSZ crystals was similar. The crystals contained elongated twin plates ~ 200 nm in cross-section. When passing through a coherent twin boundary, the lattice orientation changes. Therefore, the brightness of the image is different on different sides of the image of the boundary of the twin. The coherent boundaries of a twin have an elastic energy that is much lower than that of ordinary incoherent boundaries. The twinning plane is the {110} plane. The appearance of the twins of the monoclinic phase in 3SmSZ crystals (Fig. 1c) differed from the twins of the tetragonal phase. The twins of the monoclinic phase were rather large twin plates intersecting at an angle of 90°.

Figure 2 shows images of the structure of YSZ, GdSZ, and SmSZ crystals with a stabilizing oxide concentration of 5 mol%.

The images of twins in 5YSZ and 5GdSZ crystals change noticeably in comparison with 3YSZ and 3GdSZ crystals. With an increase in the concentration of the stabilizing oxide in YSZ and GdSZ crystals, the sizes of twins decrease. At the same time, the fields of elastic stresses present in the crystals do not allow one to clearly see the boundaries of twins. The presence of a large number of fine twins makes the structure more defective. The 5SmSZ crystals contain

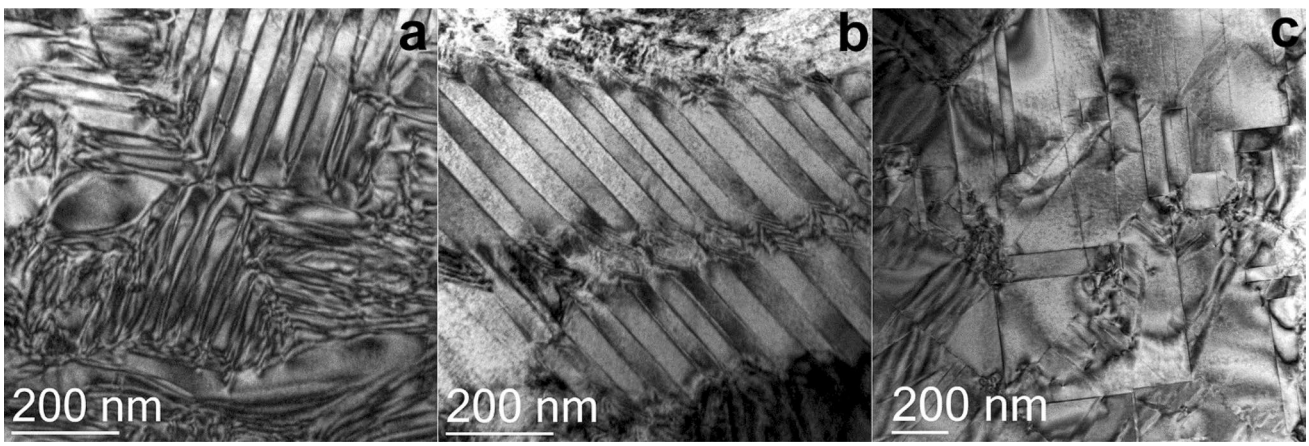

Fig. 1 TEM images of the structure of 3YSZ (**a**), 3GdSZ (**b**), and 3SmSZ (**c**) crystals

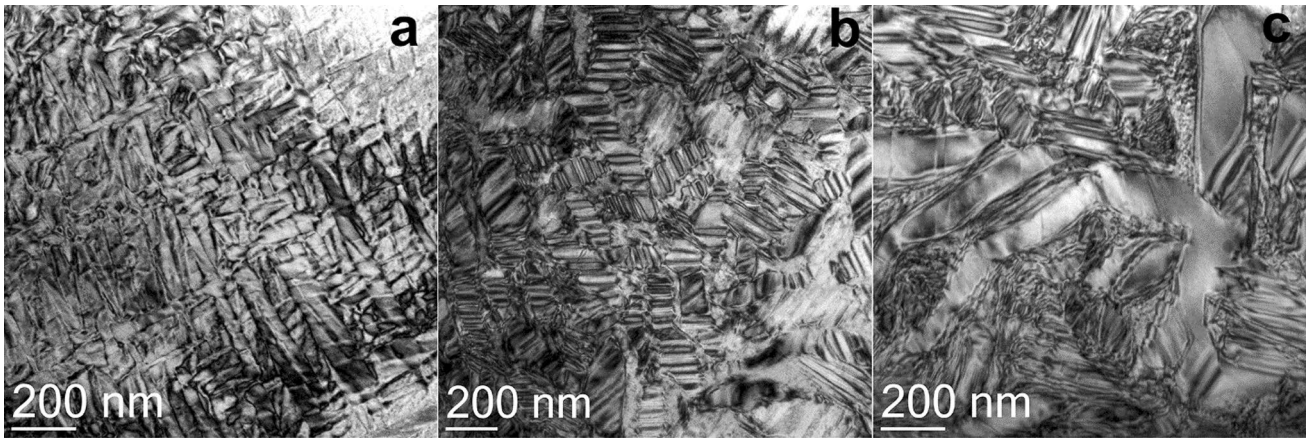

Fig. 2 TEM images of the structure of 5YSZ (**a**), 5GdSZ (**b**), and 5SmSZ (**c**) crystals

large twins whose morphology is similar to the twins in the 3YSZ and 3GdSZ crystals.

Thus, the morphology of twins in YSZ and GdSZ crystals is similar. With an increase in the concentration of stabilizing oxides, a decrease in the size of twins and the formation of a more defective structure were observed. In SmSZ crystals, even at a concentration of 5 mol%, large twins of the tetragonal phase are retained.

Microhardness and crack resistance

Table 2 shows the microhardness and crack resistance values of YSZ, GdSZ, and SmSZ crystals.

At comparable concentrations of stabilizing oxides, the values of microhardness of crystals decrease in the series $Y_2O_3 \rightarrow Gd_2O_3 \rightarrow Sm_2O_3$, which correlates with the change in interionic distances with a change in the radius of the cation of the stabilizing oxide entering the solid solution. From the studied range of compositions, the minimum value of microhardness is observed for 3SmSZ solid solutions, which may be due to the presence of a monoclinic phase in these crystals. Regardless of the type of stabilizing oxide, for all the crystals under study, the microhardness increases with an increase in the concentration of the stabilizing oxide.

For stabilizing oxide concentrations of 4 and 5 mol%, the crack resistance values increase in the series $Y_2O_3 \rightarrow Gd_2O_3 \rightarrow Sm_2O_3$. Moreover, the K_{1C} values of 4SmSZ and 5SmSZ crystals are more than twice as high as the K_{1C} values of YSZ and GdSZ crystals at comparable concentrations. Such a change in the values of crack resistance is associated with the phase composition of the crystals, namely, an increase in the amount of the transformed tetragonal phase and the degree of its tetragonality, which, in turn, increases the contribution of transformation hardening. For a concentration of stabilizing oxides of 3 mol%, this regularity does not hold. In tetragonal 3GdSZ crystals, the crack resistance values are higher than in 3YSZ crystals. However, due to the presence of the monoclinic phase, the fracture toughness of 3SmSZ crystals is lower than that of 3YSZ and 3GdSZ crystals.

With an increase in the concentration of the stabilizing oxide in the YSZ, GdSZ, and SmSZ tetragonal crystals, the crack resistance values decrease. The maximum values of crack resistance in the YSZ, GdSZ, and SmSZ crystals under study are characteristic of the 3YSZ, 3GdSZ, and 4SmSZ solid solutions, respectively. In this case, the K_{1C} values for the 4SmSZ crystal are higher than those for 3YSZ and 3GdSZ.

Table 2 Microhardness values and crack resistance of YSZ, GdSZ, and SmSZ crystals

x (mol%)	Y_2O_3		Gd_2O_3		Sm_2O_3	
	Microhardness HV, GPa	Fracture toughness K_{1C},MPa·m$^{1/2}$	Microhardness HV, GPa	Fracture toughness K_{1C},MPa·m$^{1/2}$	Microhardness HV, GPa	Fracture toughness K_{1C},MPa·m$^{1/2}$
3	13.6 ± 0.4	9.0 ± 0.3	12.5 ± 0.4	10.5 ± 0.3	9.50 ± 0.4	8.5 ± 0.3
4	14.0 ± 0.4	4.5 ± 0.3	13.4 ± 0.4	6.0 ± 0.3	12.2 ± 0.4	13.5 ± 0.3
5	14.5 ± 0.4	3.5 ± 0.3	14.0 ± 0.4	4.0 ± 0.3	12.5 ± 0.4	11.5 ± 0.3

Specific electrical conductivity

The temperature dependences of the electrical conductivity of crystals in Arrhenius coordinates are presented in Fig. 3.

It can be seen from Fig. 3 that the conductivity vs temperature functions for crystals of all the series are linear in Arrhenius coordinates. This indicates that the electrical conductivity of the crystals changes monotonically over the entire experimental temperature range. Each series of crystals is characterized by an increase in activation energy with increasing concentration of the stabilizing oxide. Thus, for YSZ and GdSZ crystals, with an increase in the concentration of the stabilizing oxide from 3 to 5 mol%, the activation energy monotonically increases from 0.87 to 0.95 eV and from 0.90 to 0.96 eV, respectively. For 4SmSZ and 5SmSZ crystals, the activation energies are 0.84 and 0.88 eV, respectively. The increase in activation energy values with increasing concentration of the stabilizing oxide from 3 to 5 mol% may be associated with the formation of a more defective twin structure in tetragonal crystals, which reduces the mobility of charge carriers. The activation energy values for SmSZ crystals are lower than for YSZ and GdSZ crystals. At the same time, larger twin sizes and a less defective structure were observed in SmSZ crystals than in YSZ and GdSZ solid solutions.

Figure 4 shows the impedance spectra of 4YSZ, 4GdSZ, and 4SmSZ crystals at a temperature of 673 K. These impedance spectra show an arc in the high-frequency region of the spectrum, reflecting volume conductivity, and a low-frequency arc caused by the polarization resistance of the electrodes. From these spectra, it is clear that the intermediate frequency arc characteristic of intergranular conduction is absent, despite the fact that all samples have a twin

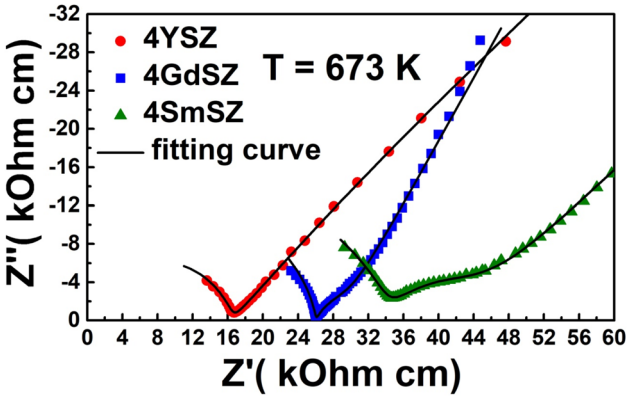

Fig. 4 Impedance spectra of the 4YSZ, 4GdSZ, and 4SmSZ crystals at 673 K

structure. Thus, we can conclude that twin boundaries do not make an additional contribution to the increase in the overall conductivity of materials. But the interaction of twins with point defects can lead to the formation of defect complexes, which reduce the mobility of oxygen vacancies and the conductivity of the material.

Figure 5 shows the dependence of specific electrical conductivity at a temperature of 1173 K on the concentration of stabilizing oxides for YSZ, GdSZ, and SmSZ crystals.

From the data presented in Fig. 5, it is clear that at a temperature of 1173 K, YSZ crystals have the highest conductivity values. The electrical conductivity values of crystals depend on the type of stabilizing oxide and decrease in the series $Y_2O_3 \rightarrow Gd_2O_3 \rightarrow Sm_2O_3$. This pattern correlates well with a change in the ionic radius of the stabilizing oxide cation, namely, with an increase in the

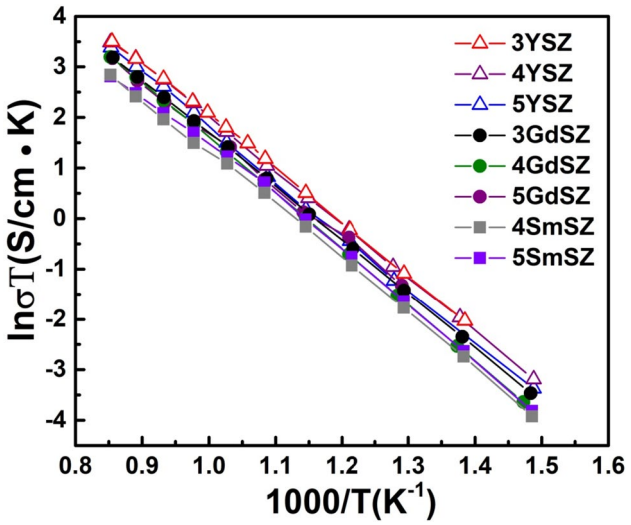

Fig. 3 Temperature dependences of electrical conductivity of YSZ, GdSZ, and SmSZ crystals

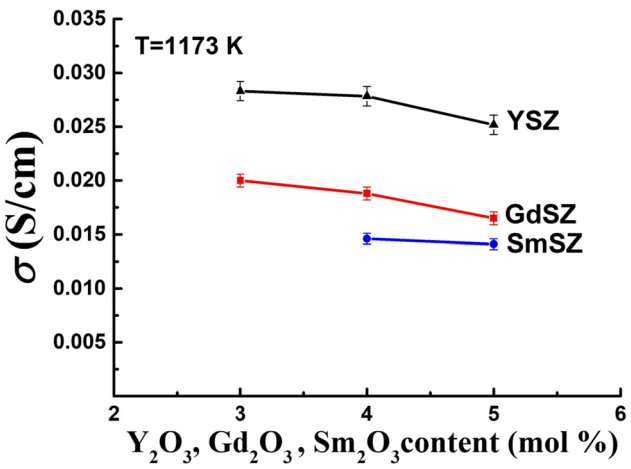

Fig. 5 Dependence of electrical conductivity at a temperature of 1173 K on the concentration of stabilizing oxides

ionic radius of the stabilizing oxide cation the conductivity of solid solutions decreases.

The conductivity of the studied crystals varies from 0.015 to 0.03 S/cm. Thus, the difference in the electrical conductivity of all the studied crystals is small, and according to the obtained conductivity values, all crystals meet the requirements for electrolytic membranes in terms of the electrical conductivity (~0.01 S/cm).

Conclusions

A comparative study of crystals of $(ZrO_2)_{1-x}(Y_2O_3)_x$, $(ZrO_2)_{1-x}(Gd_2O_3)_x$, and $(ZrO_2)_{1-x}(Sm_2O_3)_x$ solid solutions at concentrations $x = 0.03$, 0.04, and 0.05 has been carried out. It is shown that in the case of using a larger Sm^{3+} cation compared to Gd^{3+} and Y^{3+}, stabilization of the tetragonal modifications of zirconium dioxide occurs at higher concentrations of Sm_2O_3 compared to Gd_2O_3 or Y_2O_3.

At comparable concentrations of the stabilizing oxide, the amount of the transformed t-phase and the degree of its tetragonality ($c/\sqrt{2}a$) increase in the series $Y_2O_3 \rightarrow Gd_2O_3 \rightarrow Sm_2O_3$.

The twin microstructure of crystals was studied by transmission electron microscopy. With an increase in the concentration of stabilizing oxides in $(ZrO_2)_{1-x}(Y_2O_3)_x$ and $(ZrO_2)_{1-x}(Gd_2O_3)_x$ solid solutions, a decrease in the size of twins and the formation of a more defective structure were observed. In $(ZrO_2)_{1-x}(Sm_2O_3)_x$ crystals, even at a concentration of 5 mol%, large twins of the tetragonal phase are retained.

An increase in the values of crack resistance of tetragonal solid solutions in the series $Y_2O_3 \rightarrow Gd_2O_3 \rightarrow Sm_2O_3$ is shown at comparable concentrations of stabilizing oxides. The observed dependence is due to an increase in the content of the transformable tetragonal phase and the degree of its tetragonality, which make the main contribution to the mechanism of crystal hardening.

It is shown that the conductivity of all the crystals under study exceeds 0.01 S/cm at a temperature of 1173 K and thus meets the requirements for electrolytic membranes in terms of specific electrical conductivity. The conductivity of all the studied crystals varies from 0.015 to 0.03 S/cm. As the ionic radius of the stabilizing oxide cation increases, the conductivity of the solid solutions decreases. But since the value of crack resistance for tetragonal crystals $(ZrO_2)_{1-x}(Sm_2O_3)_x$ is greater than for crystals $(ZrO_2)_{1-x}(Y_2O_3)_x$ or $(ZrO_2)_{1-x}(Gd_2O_3)_x$, ZrO_2 solid solutions stabilized by Sm_2O_3 are promising and can be used as functional supporting membranes in solid oxide fuel cells.

Funding Russian Science Foundation, 22-29-01220, Nataliya Tabachkova.

References

1. Hussain S, Yangping L (2020) Review of solid oxide fuel cell materials: Cathode, anode, and electrolyte. Energy Transit 4:113–126
2. Abdalla AM, Hossain S, Azad AT, Petra PMI, Begum F, Eriksson SG, Azad AK (2018) Nanomaterials for solid oxide fuel cells: a review. Renew Sust Energy Rev 82:353–368
3. Laguna-Bercero MA (2012) Recent advances in high temperature electrolysis using solid oxide fuel cells: a review. J Power Sources 203:4–16
4. Arifin NA, Afifi AA, Samreen A, Hafriz RSRM, Muchtar A (2023) Characteristic and challenges of Scandia stabilized zirconia as solid oxide fuel cell material–in depth review. Solid State Ion 399:116302
5. Gao J, Zhao X, Cheng Z, Tian L (2023) Theoretical study on the influence of the anharmonic effect on the ionic conductivity and thermal stability of 8 mol% yttria-stabilized zirconia solid electrolyte material. Mater 16(15):5345
6. Araki W, Koshikawa T, Yamaji A, Adachi T (2009) Degradation mechanism of Scandia-stabilised zirconia electrolytes: discussion based on annealing effects on mechanical strength, ionic conductivity, and Raman spectrum. Solid State Ion 180(28–31):1484–1489
7. Badwal SPS, Ciacchi FT, Milosevic D (2000) Scandia–zirconia electrolytes for intermediate temperature solid oxide fuel cell operation. Solid State Ion 136:91–99
8. Haering C, Roosen A, Schichl H, Schnöller M (2005) Degradation of the electrical conductivity in stabilised zirconia system: Part II: Scandia-stabilised zirconia. Solid State Ion 176(3–4):261–268
9. Reveron H, Insa-Lyon MG (2020) Fourty years after the promise of «ceramic steel?»: zirconia-based composites with a metal-like mechanical behavior. J Amer Ceram Soc 103(3):1482–1513
10. Basu B (2005) Toughening of yttria-stabilised tetragonal zirconia ceramics. Int Mater Rev 50(4):239–256
11. Hannink RH, Kelly PM, Muddle BC (2000) Transformation toughening in zirconia-containing ceramics. J Amer Ceram Soc 83(3):461–487
12. Clarke DR, Oechsner M, Padture NP (2012) Thermal-barrier coatings for more efficient gas-turbine engines. MRS Bullet 37(10):891–898
13. Li Q, Hao X, Gui Y, Qiu H, Ling Y, Zheng H, Omran M, Gao L, Chen J, Chen G (2021) Controlled sintering and phase transformation of yttria-doped tetragonal zirconia polycrystal material. Ceram Int 47(19):27188–27194
14. Sourani F, Raeissi K, Enayati MH, Chu PK, SalimiJazi HR (2023) Mechanical, corrosion, and tribocorrosion behavior of biomedical ZrO_2 ceramic coatings prepared by thermal oxidation. J Mater Sci 58(9):4115–4136
15. Celik S, Timurkutluk B, Toros S, Timurkutluk C (2015) Mechanical and electrochemical behavior of novel electrolytes based on partially stabilized zirconia for solid oxide fuel cells. Ceram Int 41(7):8785–8790
16. Khajavi P, Hendriksen PV, Chevalier J, Gremillard L, Frandsen HL (2020) Improving the fracture toughness of stabilized zirconia-based solid oxide cells fuel electrode supports: effects of type and concentration of stabilizer (s). J Europ Ceram Soc 40(15):5670–5682
17. Klemensø T, Boccaccini D, Brodersen K, Frandsen HL, Hendriksen PV (2014) Development of a novel ceramic support layer for planar solid oxide cells. Fuel Cells 14(2):153–161
18. Chłędowska J, Wyrwa J, Rękas M, Brylewski T (2022) Effects of aluminum oxide addition on electrical and mechanical properties of 3 mol% Yttria-stabilized tetragonal zirconia electrolyte for IT-SOFCs. Mater 15(6):2101

19. Howard CJ, Hill RJ, Reichert BE (1988) Structures of ZrO2 polymorphs at room temperature by high-resolution neutron powder diffraction. Acta Crystallogr B Struct Sci Cryst Eng Mater 44(2):116–120
20. Basu B, Vleugels J, Van Der Biest O (2004) Transformation behaviour of tetragonal zirconia: role of dopant content and distribution. Mater Sci Eng A 366(2):338–347
21. Schelling PK, Phillpot SR, Wolf D (2001) Mechanism of the cubic-to-tetragonal phase transition in zirconia and yttria-stabilized zirconia by molecular-dynamics simulation. J Amer Ceram Soc 84(7):1609–1619
22. Simoncic P, Navrotsky A (2007) Systematics of phase transition and mixing energetics in rare earth, yttrium, and scandium stabilized zirconia and hafnia. J Amer Ceram Soc 90(7):2143–2150
23. Baither D, Baufeld B, Messerschmidt U, Foitzik AH, Rühle M (1997) Ferroelasticity of t‘-zirconia: I, high-voltage electron microscopy studies of the microstructure in polydomain tetragonal zirconia. J Amer Ceram Soc 80(7):1691–1698
24. Heuer AH (1987) Transformation toughening in ZrO_2-containing ceramics. J Amer Ceram Soc 70(10):689–698
25. Chan CJ, Lange FF, Rühle M, Jue JF, Virkar AV (1991) Ferroelastic domain switching in tetragonal zirconia single crystals—microstructural aspects. J Amer Ceram Soc 74(4):807–813
26. Chevalier J, Gremillard L, Virkar AV, Clarke DR (2009) The tetragonal-monoclinic transformation in zirconia: lessons learned and future trends. J Amer Ceram Soc 92(9):1901–1920
27. Osiko VW, Borik MA, Lomonova EE (2010) Synthesis of refractory materials by skull melting technique. In: Springer Handbook of Crystal Growth; Springer Science and Business Media LLC: Berlin/Heidelberg, Germany. 433–477
28. Niihara K (1983) A Fracture mechanics analysis of indentation-induced Palmqvist crack in ceramics. J Mater Sci Lett 2(5):221–223
29. Niihara K, Morena R, Hasselman DPH (1982) Evaluation of KIc of brittle solids by the indentation method with low crack-to-indent ratios. J Mater Sci Lett 1:13–16
30. Moradkhani A, Baharvandi H (2018) Effects of additive amount, testing method, fabrication process and sintering temperature on the mechanical properties of Al2O3/3Y-TZP composites. Eng Fract Mechan 191:446–460